01 Aug 2020

Mismatch In EBG Common-Mode Filters Implemented On PCBs

Marina Y. Koledintseva
Missouri University of Science and Technology, marinak@mst.edu

Sergiu Radu

Joseph Nuebel

Recommended Citation

M. Y. Koledintseva et al., "Mismatch In EBG Common-Mode Filters Implemented On PCBs," *IEEE Transactions on Electromagnetic Compatibility*, vol. 62, no. 4, pp. 1419 - 1429, article no. 9066900, Institute of Electrical and Electronics Engineers, Aug 2020.
The definitive version is available at https://doi.org/10.1109/TEMC.2020.2980110

Mismatch in EBG Common-Mode Filters Implemented on PCBs

Marina Y. Koledintseva, *Senior Member, IEEE*, Sergiu Radu, *Senior Member, IEEE*, and Joseph Nuebel, *Member, IEEE*

***Abstract*—In this article, impedance mismatch effects on the characteristics of common-mode (CM) electromagnetic bandgap (EBG) filters are studied using three-dimensional (3-D) full-wave numerical simulations. The CM EBG filters considered herein are designed using standard printed circuit board technology and contain either microstrip (MS) differential pairs running above the EBG plane, or stripline (SL) differential pairs running on one of the layers next to the EBG plane. First, the terminations are fixed at 50 Ω, and the effects of the differential line impedance variations on the EBG filter parameters are studied. Overall, the considered variations in the widths of the traces and edge-to-edge separation distances in both the MS and SL structures do not drastically deteriorate the performance of the EBG CM filters. Then impedances of the ports are set different from 50 Ω, and the effects of this mismatch on the baseline SL and MS EBG structures are studied. It is shown that lower port impedances may have significant effect on the characteristics of filters. In addition, baseline EBG filters are cascaded with unmatched four-port load, and this may also deteriorate performance of filters.**

***Index Terms*—Common mode (CM), differential mode (DM), electromagnetic bandgap (EBG), impedance mismatch, microstrip, notch filter, printed circuit board, stripline.**

I. Introduction

ELECTROMAGNETIC bandgap (EBG) filters can be used at the input/output (I/O) of high-speed digital electronics designs to mitigate unwanted electromagnetic emissions produced by common-mode (CM) currents [1]. EBG CM filters can work at much higher frequencies than their discrete-component and ferrite counterparts and can be directly integrated in the printed circuit board (PCB) layout without extra vias in the signal path. Data rates in digital designs steadily increase as technology develops, and therefore, there is a necessity in increasing the notch frequencies of CM filters, e.g., to 10–20 GHz, as is described in [2]–[5].

However, the more high-frequency the EBG filters, the more they are difficult to design, since the filter parameters are more sensitive to various structural and material variables [3]–[5]. Therefore, various technological features must be accounted for at the numerical simulation stages of the filter design, as it is done in [3] for microstrip (MS) EBG filters operating at 19.2 GHz, and in [4] for the 20-GHz stripline (SL) EBG filters. In [5], the comprehensive comparison of sensitivity of the MS and SL 20-GHz EBG filters to various design and material parameters is presented. A set of MS and stripline (SL) filters operating at 19–20 GHz have been designed and tested, primarily from electromagnetic compatibility (EMC) point of view, for practical use in high-speed coherency and memory links in modern servers with multiple central processing units (CPUs) [3]–[5]. From a practical standpoint, they can be implemented even directly in the package of very large and complex chips for the next generation speeds.

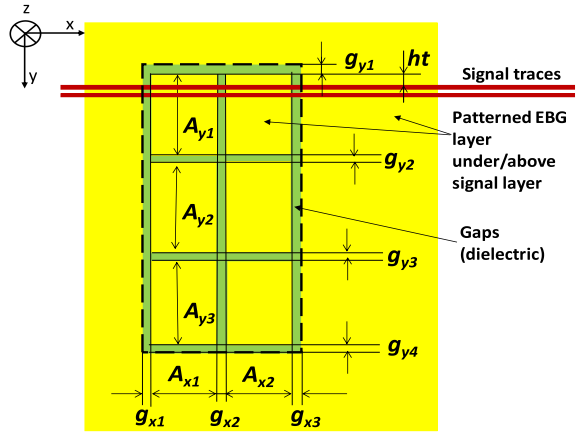

Fig. 1. Schematic of EBG structure and differential pairs running across it.

EBG structures similar to those described in [3]–[5] are shown in Fig. 1. Such an EBG structure is comprised of rectangular patches on one of the return planes (on the layer next to the signal layer). They contain a differential pair, either MS, or SL, crossing one of the EBG rows. To make a CM notch wider without compromising its depth, the patches in the rows are made of slightly different dimensions.

The characteristics of the EBG CM notch filter are the CM notch (resonance) frequency, the depth of the CM notch at the resonance frequency, the width of the CM notch at some technically sufficient level, e.g., −15 dB, minimum and maximum insertion loss (IL) for the differential mode (DM) over the frequency range of interest, or IL at the frequency of the CM

Manuscript received December 10, 2019; revised January 24, 2020, February 25, 2020, and March 5, 2020; accepted March 7, 2020. Date of publication April 14, 2020; date of current version August 13, 2020. *(Corresponding author: Marina Y. Koledintseva.)*

Marina Y. Koledintseva was with Oracle Corp., Santa Clara, CA 95054 USA. She is now with Metamagnetics, Inc., Westborough, MA 01581 USA (e-mail: mkoledintseva@mtmgx.com).

Sergiu Radu and Joseph Nuebel are with Oracle Corp., Santa Clara, CA 95054 USA (e-mail: sergiu.radu@oracle.com; joe.nuebel@oracle.com).

Color versions of one or more of the figures in this article are available online at http://ieeexplore.ieee.org.

Digital Object Identifier 10.1109/TEMC.2020.2980110

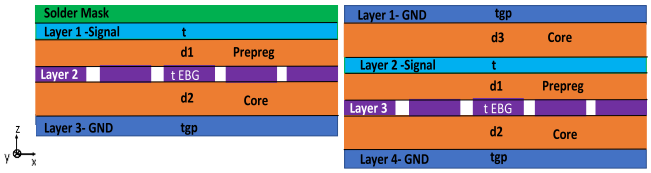

Fig. 2. Stackup of (a) microstrip and (b) single-sided stripline EBG structures.

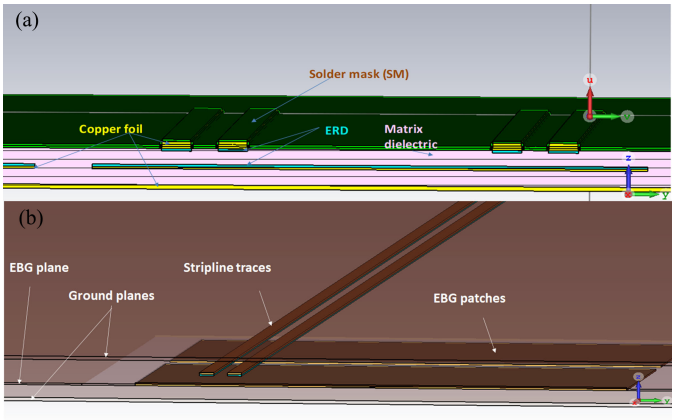

Fig. 3. Numerical (CST) models of CM EBG filters. (a) Microstrip. (b) Stripline.

notch, and the mode conversion from DM to CM or from CM to DM (these two parameters are typically the same) at the CM notch frequency and over the entire frequency range of interest.

In both MS and SL EBG filters studied in [3]–[5], the differential pairs have differential impedance close to $Z_{\mathrm{DM}} = 2Z_0 = 100\ \Omega$, and common-mode impedance is about $Z_{\mathrm{CM}} = Z_0/2 = 25\ \Omega$, while the single-ended impedance is chosen as $Z_0 = 50\ \Omega$ to match the impedance at each connector (in the designed EBG filters, the 2.92-mm coaxial connectors were used). Stackups of both filters are shown in Fig. 2.

However, due to technological variables and design constraints, line impedances may deviate from the nominal values, or there could be mismatches at the connector sides. These may affect the performance of the EBG filters. Though it is obvious that impedance mismatch may degrade filter's performance and shift notch frequency, quantification of such effects and understanding how much mismatch is still acceptable is not straightforward. Such analysis for EBG filters operating at a few dozen GHz needs to account for numerous technological features, the only feasible way of such analysis is using numerical simulations. Note that at 20 GHz these effects cannot be neglected, and any simplified mathematical and/or electrical modeling of such structures would not be accurate.

The objective of this article is to quantify how the deviation in the line impedance from the matched cases changes parameters of both MS and SL EBG CM notch filters. This study is done using the time-domain (T-solver) in commercial software 3DS Simulia CST Studio Suite [6]. The model setups are illustrated by Fig. 3. The models included various technological features (solder mask, conductor surface roughness modeled as effective roughness dielectric (ERD) [7], trapezoid shape of traces, dispersive dielectric matrix, stackup asymmetry, line length imbalance). Some of these features are indicated in Fig. 3(a). Each baseline structure (MS and SL) has been tested both experimentally and numerically [3]–[5], and the good agreement between the measured and modeled results validates the baseline models and allows for numerical experimentation. In these numerical experiments, some geometrical and/or material parameters responsible for the DM and CM impedances of the differential pairs are varied, and the resultant EBG filter parameters are retrieved for each data point of sensitivity analysis to impedance matching.

Note that the differential lines in this article are weakly and strongly coupled with the same stackup. Herein, weak coupling is assumed at $st/d_1 > 1$, and strong coupling at $st/d_1 \leq 1$, where st is the separation between the traces in the differential pair, and d_1 is the distance to the EBG plane as the closest solid return plane [8]. The proper impedance matching in the strongly coupled case cannot be achieved without using special measures for providing microwave impedance matching, *e.g.*, T- or Π-circuits, or gradual matching transformations. However, these measures for good impedance matching are not the objective for this article. The main motivation of this article is to see how the EBG filter parameters vary when the lines are not matched well enough with ports or loads. In this article [9], the impedance mismatch is provided by the deviation of width of the traces and their separation distance from the values that are close to perfect matching. The present article is an extended version of [9]. Herein, sensitivities of MS and SL filters to this way mismatched impedances are systematized and compared. Also, effects of port and load impedances variations on the parameters of CM EBG filters are added.

The methodology used in this article is based on the three-dimensional (3-D) full-wave numerical simulations well validated by measurements for baseline structures. The necessity of accounting for various technological features is critical for such high frequency of EBG CM filter as a few dozen GHz. Direct analytical or equivalent schematic electrical modeling may be unreasonably complex and still inaccurate, and therefore, they are beyond the scope of this paper.

The structure of the article is organized as follows. Sections II and III contain the study of impedance mismatch effects of EBG filter parameters in MS and SL cases, respectively, when widths of the signal traces and separation distances between them in differential pairs vary. Mismatched ports and load effects on the performance of the baseline EBG filters are discussed in Sections IV and V, respectively. Finally, Section VI concludes this article.

II. Study of Impedance Mismatch Effects in Microstrip EBG Filters

The intended for 19.2 GHz CM notch filter responses of the tested MS EBG structure are shown in Fig. 4. The data for both CM and DM modeled in CST Studio with different technological features and the corresponding measured results closely agree, and this validates the model.

The existing model was adjusted to shift the resonance closer to 20 GHz (see the black dotted lines) to provide the "baseline" structure. The intention herein is to further have both

TABLE I
PARAMETERS OF MICROSTRIP EBG FILTERS

Filter	Ay, mm	Ax, mm	Gap, mm	Offset from top ht, mm	Trace width wt, mil (mm)	Separation st, mil (mm)	Dielectric Layer d1, mil (mm)	Dielectric Layer d2, mil (mm)
Modeled	A_{y1} =3.78 A_{y2} =3.82 A_{y3} =3.86	A_{x1} = 1.91 A_{x2} =1.91	g_x=0.39 g_y=0.39	ht=0.472	wt=7.1 mil (0.18 mm)	st=7.99 mil (0.203 mm)	d_1=5.118 mil (0.13 mm)	d_2=3.937 mil (0.1 mm)
Measured	A_{y1} =3.78 A_{y2} =3.82 A_{y3} =3.86	A_{x1} = 1.91 A_{x2} =1.91	g_x=0.39 g_y=0.39	ht=0.472	wt=7.1 mil (0.18 mm)	st=7.99 mil (0.203 mm)	d_1=5.118 mil (0.13 mm)	d_2=3.937 mil (0.1 mm)
Adjusted Baseline	**A_{y1} =3.60** **A_{y2} =3.65** **A_{y3} =3.74**	A_{x1} = 1.91 A_{x2} =1.91	g_x=0.39 g_y=0.39	ht=0.472	wt=7.1 mil (0.18 mm)	st=7.99 mil (0.203 mm)	d_1=5.118 mil (0.13 mm)	d_2=3.937 mil (0.1 mm)

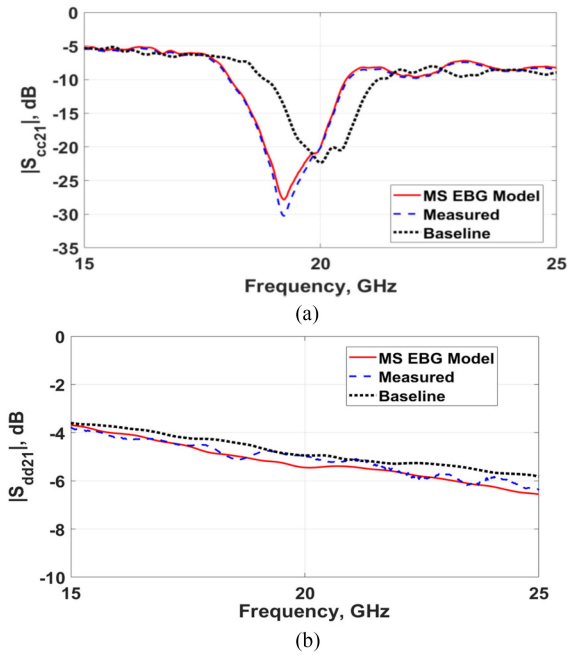

Fig. 4. Modeled and measured and frequency responses of microstrip CM EBG notch filter insertion loss for (a) CM and (b) DM.

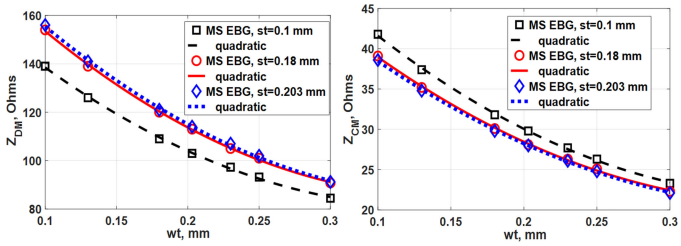

Fig. 5. Dependencies of MS differential pair impedances Z_{DM} and Z_{CM} on the widths of the lines wt for different edge-to-edge separation distances st.

baseline MS and SL structures with as close as possible CM notch (resonance) frequencies when considering and comparing sensitivities to mismatch effects. Then, the parameters of the models will be varied so that it would be possible to compare the MS and SL EBG filters in terms of their sensitivity to impedance mismatch.

Geometrical parameters of the modeled, measured, and adjusted baseline MS filters are given in Table I. The first row of rectangular patches in the modeled and measured 19.2-GHz 2×3 EBG pattern has the dimension $A_{y1} = 3.78$ mm, and the other two rows have $A_{y2} = 3.82$ mm and $A_{y3} = 3.86$ mm; the dimension along the x-axis (along the wave propagation) is $A_{x1} = A_{x2} = 1.91$ mm in all the patches. The 20-GHz baseline MS filter has slightly smaller dimensions. They are $A_{y1} = 3.60$ mm, $A_{y2} = 3.65$ mm, $A_{y3} = 3.74$ mm, and the width of all the patches along the x-direction is the same as in the 19.2-GHz filter, $A_{x1} = A_{x2} = 1.91$ mm. The gaps between all the patches are the same in both 19.2-GHz and 20-GHz filters, $g_x = g_y = 0.39$ mm. Differential pairs in both filters are running at the same distance $ht = 0.472$ mm from the top edge of the first row on the EBG. Geometrical parameters of the lines in both filters are the same—trace width is $wt = 7.1$ mil (0.18 mm); separation distance is $st = 7.99$ mil (0.203 mm); dielectric thickness between the top layer with MS lines and EBG layer is $d_1 = 5.118$ mil (0.13 mil); and thickness of dielectric between the EBG layer and the ground (return) plane is $d_2 = 3.937$ mil (0.1 mm). Lengths of the MS differential pairs are identical in the original modeled and the baseline structure and are equal to $L = 80.4$ mm. The PCB dielectric (Megtron 6) is modeled with dielectric constant $DK = 3.6$ and dissipation factor $DF = 0.0073$ taken at 35 GHz (modeled in CST Studio with constant fit). Solder mask is modeled on top of the filters with the following parameters: $\varepsilon'_{sm} = 3.55$ and $\tan\delta_{sm} = 0.020$, and thickness of the SM is $t_{sm} = 0.6$ mil $= 0.0153$ mm. All filters are also modeled with conductor having standard (STD) copper foil profile. Foil thickness on the signal layer is 1 oz + 0.3 oz plating, ground planes are 1 oz copper. Copper foil surface roughness is represented as ERD having $\varepsilon_{\mathrm{rough}}{}' = 12$ and $\tan\delta_{\mathrm{rough}} = 0.17$ and thickness $T_r = 0.5$ mil $= 13$ μm on the rougher (matte) side only [9], both on traces and return plane(s).

Ranges of the modeled impedance values for MS EBG filters are calculated as in [10]. They are summarized in Table II and illustrated by Fig. 5 that correlates width of traces and their separation with differential-mode Z_{DM} and common-mode Z_{CM} impedances on the lines.

For the modeled MS differential pairs with the given dielectric height $d_1 = 0.13$ mm, the differential impedance Z_{DM} decreases from 140 Ω at $wt = 0.1$ mm to 84.8 Ω at $wt = 0.3$ mm for the lowest separation distance of $st = 0.1$ mm (strongly

TABLE II
MODELED RANGES OF IMPEDANCES OF MICROSTRIP EBG FILTERS

Coupling	Z DM min, Ω	Z DM max, Ω	Z CM min, Ω	Z CM max, Ω
Loosely coupled (st=0.203 mm)	92.3 (at wt=0.3 mm)	157 (at wt=0.1 mm)	22.2 (at wt=0.3 mm)	39.0 (at wt=0.1 mm)
Intermediate (st=0.18 mm)	91.2 (at wt=0.3 mm)	155 (at wt=0.1 mm)	22.3 (at wt=0.3 mm)	39.5 (at wt=0.1 mm)
Strongly coupled (st=0.1 mm)	84.8 (at wt=0.3 mm)	140 (at wt=0.1 mm)	23.4 (at wt=0.3 mm)	41.8 (at wt=0.1 mm)
Baseline (st=0.203 mm)	119 (at wt=0.18 mm)		27.9 (at wt=0.18 mm)	

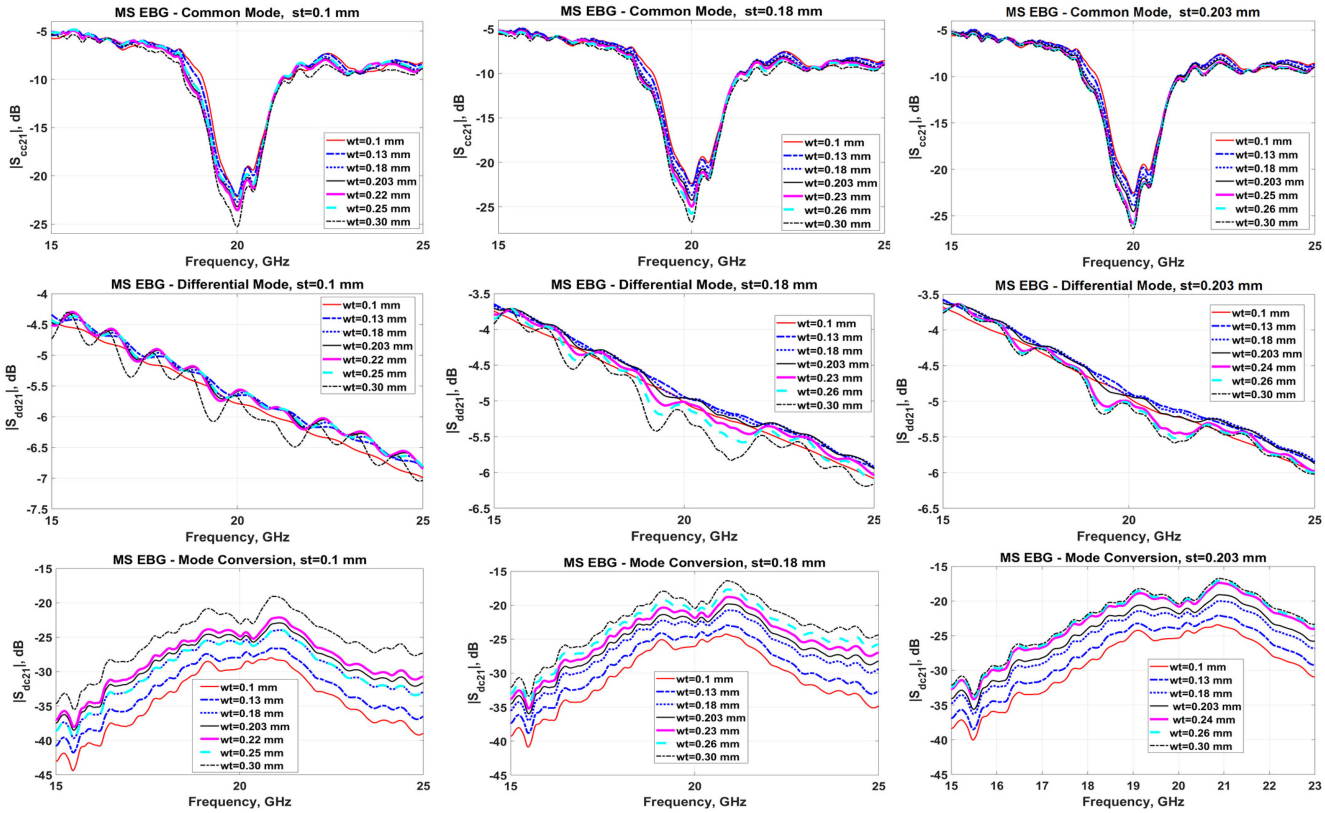

Fig. 6. MS EBG filter frequency responses in terms of mixed-mode *S*-parameters for different widths of traces *wt* and edge-to-edge separation distances *st*.

coupled case). The corresponding CM impedance Z_{CM} varies from 41.8 Ω at $wt = 0.1$ mm to 23.4 Ω at $wt = 0.3$ mm. For the weakly-coupled lines with $st = 0.18$ mm, the impedance Z_{DM} changes from 155 Ω to 91.2 Ω, and the impedance Z_{CM}varies from 39.5 Ω to 22.3 Ω for the same range of *wt*. For the more loosely coupled lines with $st = 0.203$ mm, Z_{DM} ranges from 157 Ω to 92.3 Ω, and Z_{CM} varies from 39 Ω to 22.2 Ω.

The MS EBG filter frequency responses in terms of mixed-mode *S*-parameters (CM, DM, and mode conversion) for different widths of MS traces *wt* and their edge-to-edge separation distances *st* are shown in Fig. 6. With $d_1 = 0.13$ mm, the case of $st = 0.1$ mm corresponds to the strongly coupled differential pair, and the two other cases, $st = 0.18$ mm and 0.203 mm,—to the weakly coupled traces. It is seen from Fig. 6 that the most mismatched case (in terms of impedance) with $wt = 0.30$ mm for all *st* values results in the deepest CM notch, highest insertion loss for DM, and the worst mode conversion. The CM notch frequency is not very sensitive to mismatch; it just slightly moves to the lower frequencies as *wt* increases.

The CM EBG filter characteristics—notch frequency, depth, and width at −15 dB level as functions of the microstrip trace width *wt* for a number of different separation distances between the traces of the differential pair *st* are summarized in Fig. 7. The data corresponding to the baseline filter is indicated in this figure, too.

Note that the modeled cases with $st = 0.18$ mm and 0.203 mm corresponding to the weak coupling in the MS differential pair, and $st = 0.1$ mm corresponding to the strong-coupled case, are all pretty close to the borderline criterion $st/d_1 = 1$, and therefore, the overall behavior is not very strongly affected by whether coupling is "weak" or "strong" in the studied cases. If there were $st/d_1 > 3$, the coupling would have been less than

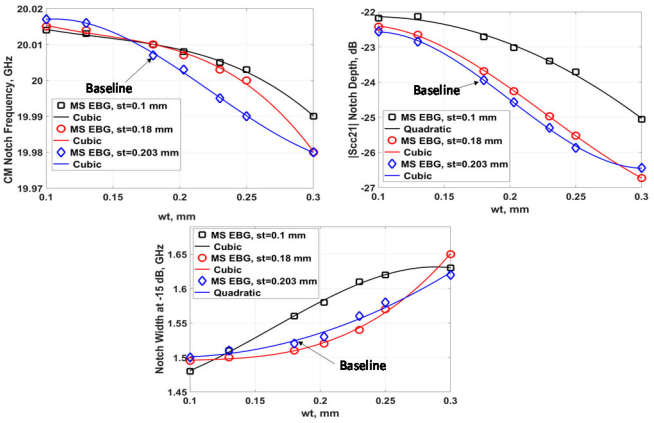

Fig. 7. Dependencies of MS EBG filter characteristics on the widths of the lines of MS differential pairs for different edge-to-edge separation distances.

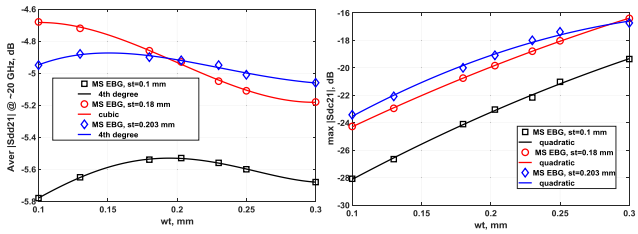

Fig. 8. Average $|\mathrm{Sdd}_{21}|$ at around 20 GHz and maximum $|\mathrm{Sdc}_{21}|$ as functions of the widths of the lines for different edge-to-edge separation in MS case.

2%, and then the more significant difference would have been seen.

Note that actually the 20-GHz baseline structure with the stackup exactly the same as in the real fabricated design is not perfectly matched, having $Z_{\mathrm{DM}} = 119\ \Omega$ and $Z_{\mathrm{CM}} = 27.9\ \Omega$. The 100-Ω DM impedance is satisfied for $wt = 0.22$ mm, when $st = 0.1$ mm, and is also very close to 100 Ω, when the width trace is about $wt = 0.26$ mm for both cases of $st = 0.18$ mm and $st = 0.203$ mm. The CM impedances in these cases are very close to 25 Ω. The impedance-matched data points fall within the modeled ranges shown in Figs. 6–8.

Fig. 6 shows that the CM $|\mathrm{Scc}_{21}|$ notch is surprisingly robust with respect to the technological variations of widths of tracs and separation between them. This is because the CM $|\mathrm{Scc}_{21}|$ notch frequency and depth are fundamentally dependent of the patch geometry and dielectric [1]. Whatever is done to the lines in small range of variations will only slightly affect the coupling to the EBG patches. However, $|\mathrm{Sdd}_{21}|$ and $|\mathrm{Scd}_{21}|$ depend almost entirely on the differential line characteristics. Therefore, they will be affected by the abovementioned technological variations. Also, it is seen that $|\mathrm{Sdd}_{21}|$ is best for weak coupling, and weak coupling is most widely used in practical designs for signal integrity (SI) purposes [8]. The $|\mathrm{Sdc}_{21}|$ is always below 15 dB, and this is not a concern from practical EMC/SI points of view.

According to Fig. 7, the CM EBG notch frequency monotonically reduces as *wt* increases from 0.1 mm to 0.3 while the separation *st* is constant; also, as *wt* increases, the impedance Z_0 decreases. The baseline data is in between the maximum and minimum impedances studied in this article. Note that the reduction of the notch frequency with the increase of *wt* is insignificant for all three cases of *st*, both weakly and strongly coupled differential pairs.

The CM notch depth increases that shows the lower negative dB values as the parameter *wt* increases. The two weakly-coupled cases appear to be very close to each other, while the stronger-coupled case has the lower notch depth than the two weakly-coupled cases. However, from CM suppression point of view, the value at the resonance frequency does not matter much; the typical requirement is the suppression over some bandwidth at the level, e.g., −15 dB, and the required bandwidth of greater than 1 GHz is satisfied in all the studied cases, as the third set of the plots in Fig. 7 shows. It is seen that the CM notch width at the level of −15 dB increases with *wt*. The dependencies of the notch width on *wt* are almost identical for the two weakly-coupled cases, while the behavior for the strongly coupled case is different. The width of the notch is slightly higher for the strongly coupled case, and it grows faster for the lower *wt* values and then slows down for $wt > 0.25$ mm.

Fig. 8 shows the behavior of average DM at around 20 GHz and maximum mode conversion that takes place at frequencies close to 20 GHz (simulations were run from d.c. to 30 GHz).

Overall, the sensitivity of the CM EBG microstrip filter performance to the line impedance mismatch is not significant. Impedance mismatch caused by variations in the trace width and edge-to-edge separation in the MS differential pair does not cause any significant degradation in the EBG filter performance. On the contrary, the CM notch width slightly increases (by about 100 MHz) as the DM and CM impedances decrease in the considered ranges of trace widths and separation distances between the traces. Therefore, slight deviation of the MS line impedances (within ±25%) from the nominal should not be a problem for an EBG filter design.

III. Study of Impedance Mismatch Effects in Stripline EBG Filters

The modeled in CST Studio and measured CM EBG notch filter responses for the tested SL structure, for both CM and DM, are shown in Fig. 9. The EBG patch geometry in this case provides the CM notch close to 20 GHz (slightly higher). Port effects at the connectors, including via stub artifacts, were removed from the measurements [5].

There is just a slight difference in DM insertion loss in the original modeled structure, corresponding to the measured one, and the baseline due to the slight difference in the dielectric loss tangent that was set in the model to match the measured results with the removed port effects. The geometrical data for the modeled, measured, and adjusted baseline SL EBG filters are given in Table III. Dimensions of the patches in the 2 × 3 SL EBG filter are the same as for the MS EBG structure, i.e., $A_{y1} = 3.60$ mm, $A_{y2} = 3.65$ mm, $A_{y3} = 3.74$ mm, and $A_{x1} = A_{x2} = 1.91$ mm. Gap sizes are also the same as in the MS case, $g = 0.39$ mm. The EBG patches are crossed by the SL differential pair at the same distance as the MS differential pair crosses its

TABLE III
INITIAL PARAMETERS OF STRIPLINE EBG FILTERS

Filter	Ay, mm	Ax, mm	Gap, mm	Offset from top ht, mm	Trace width wt	Separation st	Dielectric layer d1, mil (mm)	Dielectric layer d2, mil (mm)	Dielectric Layer d3, mil (mm)
Modeled	A_{y1} =3.78 A_{y2} =3.82 A_{y3} =3.86	A_{x1} = 1.91 A_{x2} =1.91	g_x=0.39 g_y=0.39	ht=0.472	wt=4.1 mil (0.104 mm)	st=3.937 mil (0.1 mm)	d_1=3.937 mil (0.1 mm)	d_2=4.488 mil (0.114 mm)	d_3=4.331 mil (0.11 mm)
Measured	A_{y1} =3.78 A_{y2} =3.82 A_{y3} =3.86	A_{x1} = 1.91 A_{x2} =1.91	g_x=0.39 g_y=0.39	ht=0.472	wt=4.1 mil (0.104 mm)	st=3.937 mil (0.1 mm)	d_1=3.937 mil (0.1 mm)	d_2=4.488 mil (0.114 mm)	d_3=4.331 mil (0.11 mm)
Adjusted Baseline	**A_{y1} =3.60** **A_{y2} =3.65** **A_{y3} =3.74**	A_{x1} = 1.91 A_{x2} =1.91	g_x=0.39 g_y=0.39	ht=0.472	**wt=3.7 mil (0.094 mm)**	st=3.937 mil (0.1 mm)	d_1=3.937 mil (0.1 mm)	d_2=4.488 mil (0.114 mm)	d_3=4.331 mil (0.11 mm)

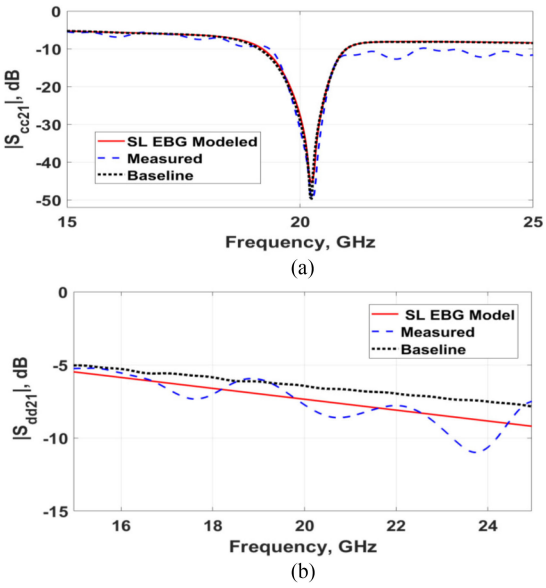

Fig. 9. Measured and modeled frequency responses of stripline CM EBG notch filter insertion loss for (a) CM and (b) DM.

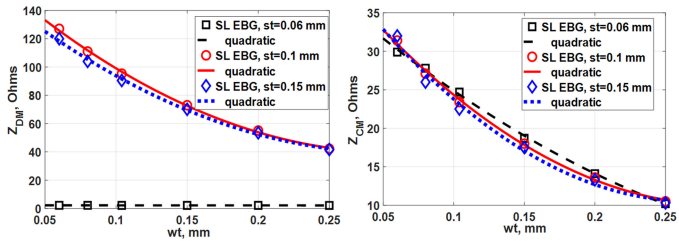

Fig. 10. Dependencies of SL differential pair impedances Z_{DM} and Z_{CM} on the widths of the lines wt for different edge-to-edge separation distances st.

EBG, $ht = 0.39$ mm. The modeled baseline SL EBG structure is geometrically the same as the one that is modeled and measured.

The thickness of the dielectrics between the signal layer and the EBG layer is $d_1 = 0.1$ mm, between the EBG and the next-layer ground plane is $d_2 = 0.114$ mm, and between the signal layer and the other ground plane above is $d_3 = 0.11$ mm. The width of the signal traces in the baseline structure is $wt = 0.104$ mm, and the edge-to-edge separation between the traces is $st = 0.10$ mm. The prepreg and core of Megtron 6 in the baseline structure are modeled with identical parameters, and in the CST model they are the same as in the MS structure: $DK = \varepsilon_r' = 3.6$ and $DF = \tan\delta = 0.0073$ set as constant fit at 35 GHz. Lengths of the SL differential pairs are also the same as in the MS structure, $L = 80.4$ mm. Copper foil on the signal layer is 0.5 oz, and 1 oz on the ground planes.

Impedances of the SL pairs crossing the EBG are varied by varying the trace width wt and separation distance st, similar to the numerical experiments for the MS EBG structure. In these experiments, Z_{DM} and Z_{CM} vary over some range that includes the SL baseline structure. Ranges of the modeled impedance values for SL EBG filters are calculated using [10] and given in Table IV. Fig. 10 correlates impedances for SL differential pairs with widths of traces and separation between them.

The baseline differential impedance is $Z_{DM} = 102\ \Omega$, and common-mode impedance is $Z_{CM} = 25\ \Omega$ for the traces of the width $wt = 0.094$ mm and separation distance $st = 0.1$ mm. This is very close to the matched-impedance case. For the separation distance $st = 0.15$ mm (weak coupling), the maximum $Z_{DM} = 120\ \Omega$ and $Z_{CM} = 29.9\ \Omega$ for the trace width of $wt = 0.06$ mm, and the minimum $Z_{DM} = 41.7\ \Omega$ and $Z_{CM} = 20.8\ \Omega$ for $wt = 0.25$ mm.

For the separation distance, corresponding to strong coupling in the SL differential pair, $st = 0.06$ mm, the $Z_{DM} = 2.21\ \Omega$ and $Z_{CM} = 33.2\ \Omega$ for $wt = 0.06$ mm, and $Z_{DM} = 2.17\ \Omega$ and $Z_{CM} = 10.8\ \Omega$ for $wt = 0.25$ mm.

The modeled filter responses for these ranges of differential pair geometries and, hence, impedances, are presented in Figs. 11 and 12. Fig. 11 shows frequency dependencies of mixed-mode parameters for SL EBG filters, insertion loss for common-mode, DM, and mode conversion, as functions of frequency for various wt and st parameters. Impedance mismatch effect is seen in Fig. 11 very well. For the most mismatched case with $wt = 0.25$ mm for all the three modeled separation distances st, the insertion loss for DM is the highest, mode conversion is also the highest, i.e., the worst. As for the CM notch, it is the lowest for $st = 0.06$ mm and $st = 0.1$ mm, but not for $st = 0.15$ mm (loosely coupled SLs). However, the CM notch frequency is the lowest for all the cases with $wt = 0.25$ mm. The

TABLE IV
MODELED RANGES OF IMPEDANCES OF STRIPLINE EBG FILTERS

Coupling	Z DM min, Ω	Z DM max, Ω	Z CM min, Ω	Z CM max, Ω
Loosely coupled (st=0.15 mm)	41.7 (at wt=0.25 mm)	120 (at wt=0.06 mm)	10.3 (at wt=0.25 mm)	29.9 (at wt=0.06 mm)
Intermediate (st=0.1 mm)	42.2 (at wt=0.25 mm)	127 (at wt=0.06 mm)	10.5 (at wt=0.25 mm)	31.4 (at wt=0.06 mm)
Strongly coupled (st=0.06 mm)	2.17 (at wt=0.25 mm)	2.21 (at wt=0.06 mm)	10.8 (at wt=0.25 mm)	33.2 (at wt=0.06 mm)
Baseline (st=0.1 mm)	102 (at wt=0.094 mm)		25 (at wt=0.094 mm)	

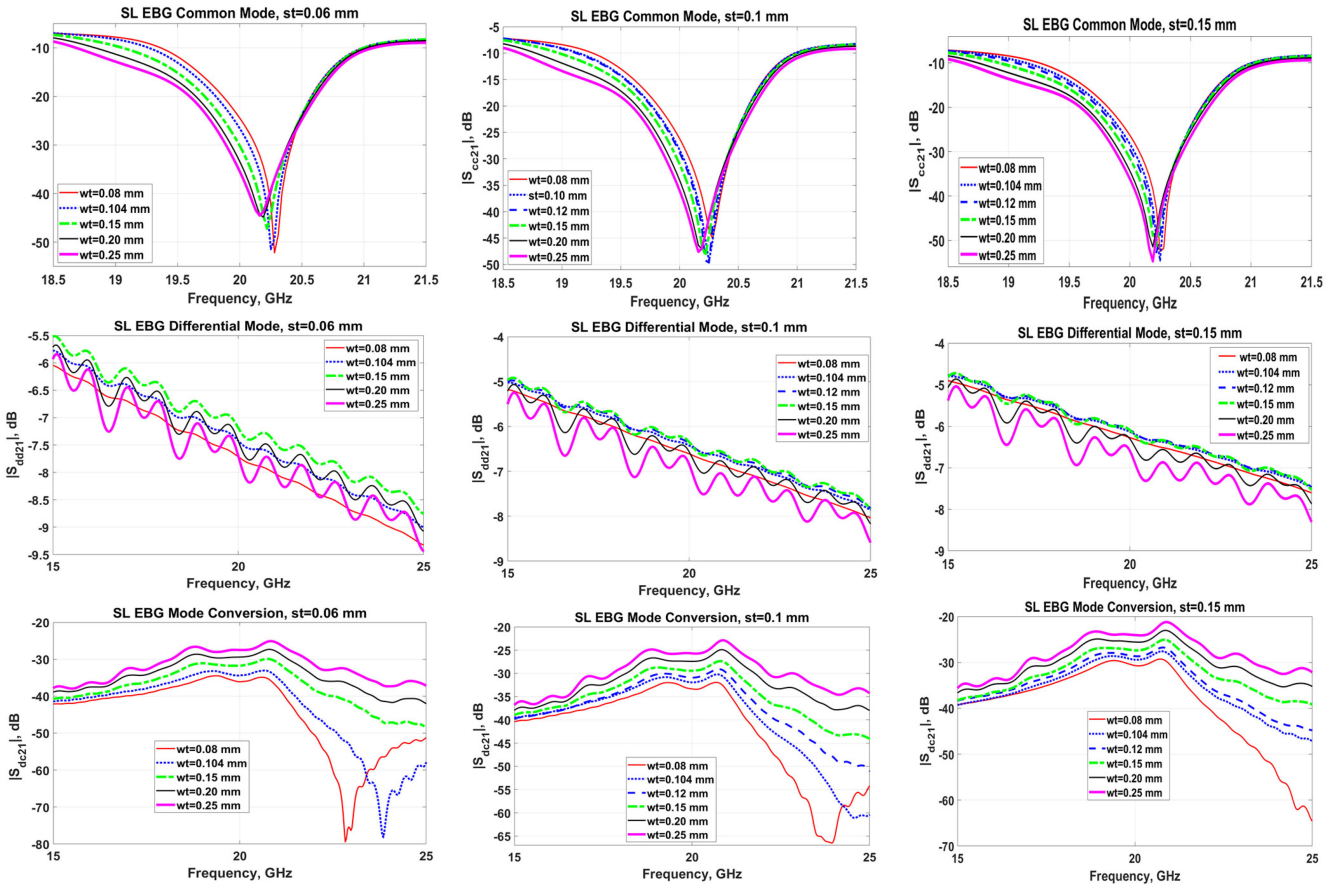

Fig. 11. SL EBG filter frequency responses in terms of mixed-mode *S*-parameters for different widths of traces *wt* and edge-to-edge separation distances *st*.

best matched cases show the deepest CM notch, the smoothest and almost the lowest IL for the DM, and mode conversion is almost the best over the frequency range of interest. Fig. 12 shows the trends of CM SL EBG filter parameters (CM notch frequency, depth, and width at −15 dB level) as functions of *wt* for a number of *st* values. The cases with $st = 0.1$ mm and 0.15 mm correspond to the weakly-coupled, and $st = 0.06$ mm to the strongly coupled differential pairs. Fig. 13 illustrates DM at around 20 GHz and maximum mode conversion trends verus traces width and separation.

The trace width increase in the SL cases results in the larger CM notch shift to the lower frequencies as compared to the MS EBG filters. This is related to the wider range of impedances for the lines considered in the SL case. The CM notch depth in the SL case decreases as *wt* increases, as opposed to the MS case, where the notch depth increased with *wt*. In the MS case, the increased loss at the notch is related to the increased reflection that results in less transmission along the differential pair as *wt* increases and CM impedance reduces. The mode structure in the MS line is much more complex than in the SL line; in the latter, the electromagnetic field is closer to the pure transverse electromagnetic wave (TEM) wave. The CM notch width in the MS case increased accordingly. However, in the SL case, as *wt* increases and mismatch significantly increases, the notch becomes less deep. The stronger mismatch creates multiple reflections and increased loss on the transmission line. Also, a part of the

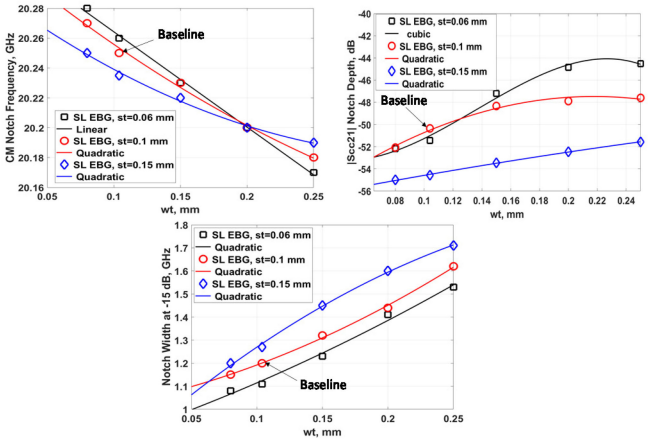

Fig. 12. Dependencies of SL EBG filter characteristics on the widths of the lines of SL differential pairs for different edge-to-edge separation distances.

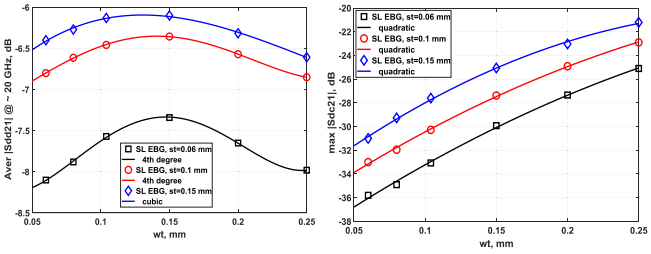

Fig. 13. Average $|\mathrm{Sdd}_{21}|$ at around 20 GHz and maximum $|\mathrm{Sdc}_{21}|$ as functions of the widths of the lines for different edge-to-edge separation in SL case.

reflected energy is better concentrated and absorbed by the ERD layer, not letting it to resonate in the EBG cavity, and hence, the notch at the resonance frequency is less deep. The SL filter notch width increases with *wt*, and this is similar to the MS filter, but the range of the notch widths is greater in the SL case. The resulting CM notch width for the strongly coupled SL differential pair is slightly lower than for the weakly-coupled cases, but the slopes of the notch width increase are almost the same for all the three modeled cases. The notch depth is the largest for the most weakly-coupled case, and the lowest for the most strongly coupled one. This is due to the more "loaded" resonance, i.e., stronger interaction between the traces and the cavity, when coupling between the differential lines exciting the EBG structure is stronger.

Similar to the MS cases, the deviation from the nominal impedances in the SL differential pair does not drastically degrade the performance of the EBG filter, other than shifting the CM notch to the lower frequencies as the width of the traces increases. The notch width, which is the most important parameter for the CM notch filter, even increases as the trace width increases, or impedance mismatch increases.

The best matched case is in between the considered lowest and highest trace widths. The strongly mismatched cases have not been considered herein, since it is obvious that this may significantly deteriorate the EBG filter performance. Only sensitivity to slight variation of geometrical parameters of filters close to the typical technological deviations around the matched cases are of interest.

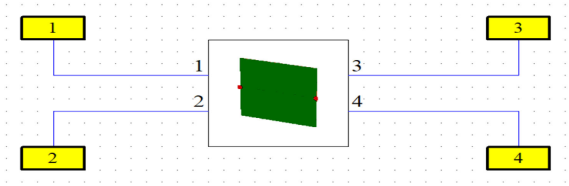

Fig. 14. 4-port network representing a modeled EBG structure and external ports with identical impedances set in the numerical experiments.

IV. Impedance Mismatch Between EBG Filters and Network Ports

Herein, we investigate how important matching of the EBG filter with the port impedances of the network. *S*-parameters (TouchStone s4p files) for the EBG baseline MS and SL filters were previously obtained from numerical simulations in CST Studio.

Then the external ports with different assigned impedances were attached to the four-port network in the CST schematics canvas as is shown in Fig. 14. Note that since the resultant single-ended s4p parameters are then converted to mixed-mode ones, all the ports have to be assigned identical impedances. The numerical experiments with mismatched ports are shown in Fig. 15 for both MS and SL EBG structures. It is seen that the lower port impedances cause more CM notch widening and deterioration and higher loss for DM and CM. Mode conversion also reduces as port impedances reduce. The trends of filter parameters are summarized in Figs. 16 and 17.

When impedance of ports increases above 50 Ω, CM notch and mode conversion practically do not change. Indeed, the higher the port terminations, the "cleaner" the $|Scc_{21}|$.

It is also seen that for the MS structure, the notch is the deepest and the widest with the lowest termination (10 Ω). Since $|Scc_{21}|$ is fundamentally a function of patch geometry and dielectric, port termination will affect only the coupling coefficient between traces and patches. This indicates that the higher the current in the traces (at the lower port impedance), the deeper the CM node. Therefore, the H-field plays part in this coupling. On the other hand, as the terminations increase from 50 to 100 Ω, the CM notch appears to be unaffected. This suggests that at the lower current (at the higher port impedance) the E-field play a bigger role in coupling and maximum coupling is achieved around 50 Ω.

Ports mismatch affects the DM causing the standing wave behavior and transmission loss. The $|Sdd_{21}|$ is the worst with the lowest termination (10 Ω), which suggests that the losses on the line are more current and H-field dependent for the lower termination. However, the $|Sdd_{21}|$ trend appears to be reversed for 60–100 Ω. Up to 50 Ω, the worst is 10 Ω. Above 50 Ω, the worst is 100 Ω. This indicates that for $|Sdd_{21}|$ the higher mismatch is worse, which is related to the higher voltage standing wave ratio (VSWR) on the line. However, this is not the case for $|Scc_{21}|$: as is discussed earlier, the CM notch is comparatively robust to ports

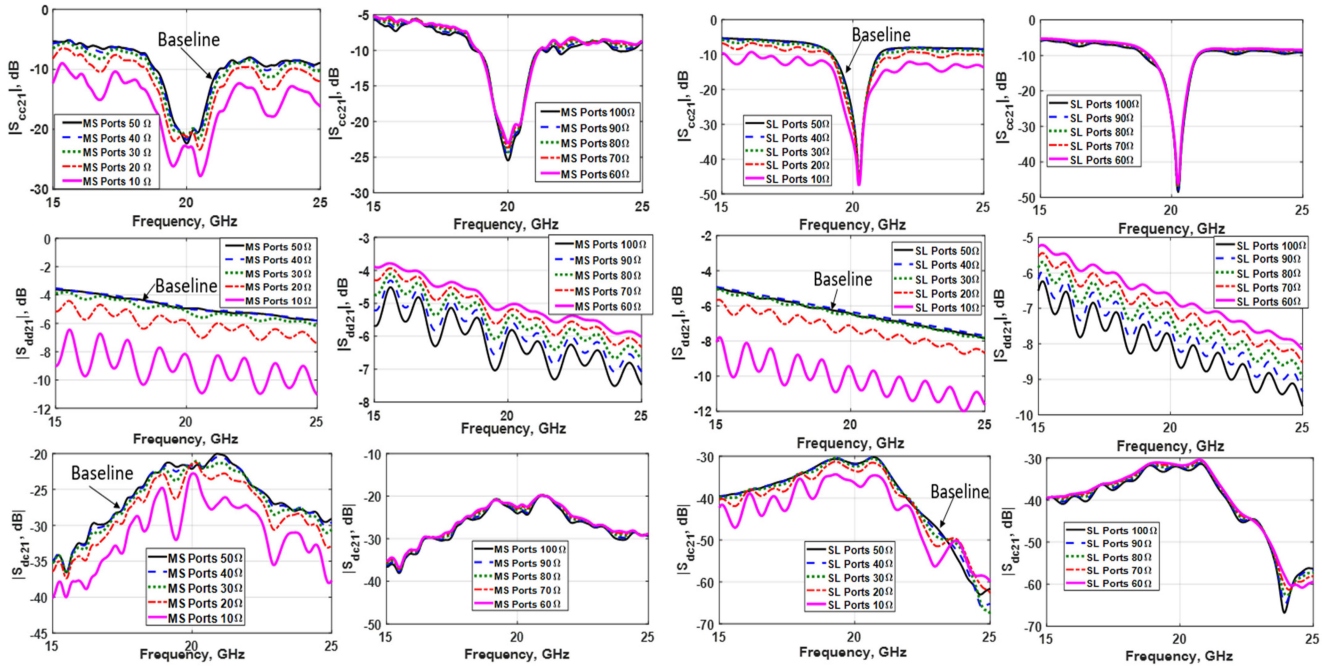

Fig. 15. Effect of ports impedance in the network of the baseline EBG filters on the CM, DM, and mode conversion performance. Two left-hand columns correspond to MS EBG filter, and two right-hand columns correspond to SL EBG filter.

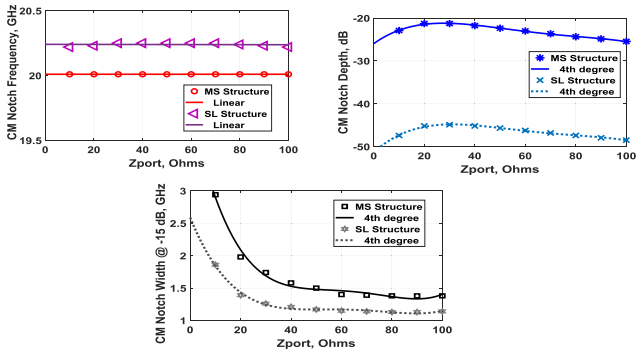

Fig. 16. CM EBG filter basic parameters (CM notch frequency, depth, and width) trends versus impedance of ports in the network.

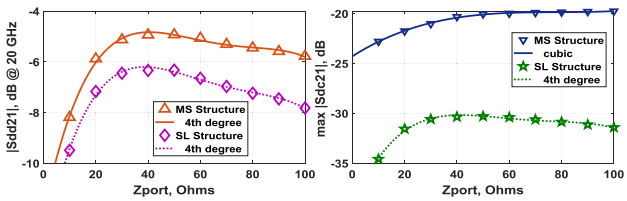

Fig. 17. CM EBG filter average $|S_{dd21}|$ around 20 GHz and maximum mode conversion behavior vs. impedance of ports in the network.

mismatch. As for the mode conversion, the behavior of $|Sdc_{21}|$ consistent with that of $|Scc_{21}|$, because the better coupling to the patch is associated with lower mode conversion, especially for low terminations. It is also seen that ports mismatching has slightly stronger effect on the MS EBG structure than on the more robust SL EBG structure.

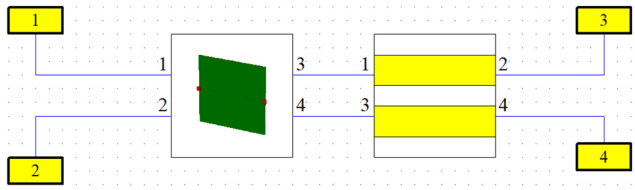

Fig. 18. Four-port network representing a modeled EBG structure cascaded with a lossless mismatched network of coupled transmission line.

V. Impedance Mismatch of EBG Filters With Load

Modeling experiments are also run for both MS and SL EBG structures loaded (cascaded) with a transmission line (TL) block of lossless coupled transmission lines available in CST schematics canvas (see Fig. 18). The default length of these lines is 5 mm and dielectric constant for both even and odd modes is 9.9. The external ports are all set as 50 Ω.

The results of modeling are shown in Fig. 19. The baseline cases without load are given for comparison. It is seen that when the CM impedance of the load block is $Zcm = 25\ \Omega$ and DM impedance is $Zdm = 100\ \Omega$ (nominal case), the resultant CM notches, DM, and mode conversion values of the entire four-port network are close to the initial unloaded case. Therefore, external matching of both MS and SL EBG structures with the rest of the network are very important. In practice, if an EBG filter is used at the I/O port, the TL block as the one modeled herein, represents a transition to the cable. Typically, this is a connector with all the problems related to pin escapes and slightly different impedance. This means that a poorly matched TL block may deteriorate the EBG performance, i.e., impair the CM notch and result in unacceptable DM loss. Therefore, carefully choosing the connector and paying attention to its

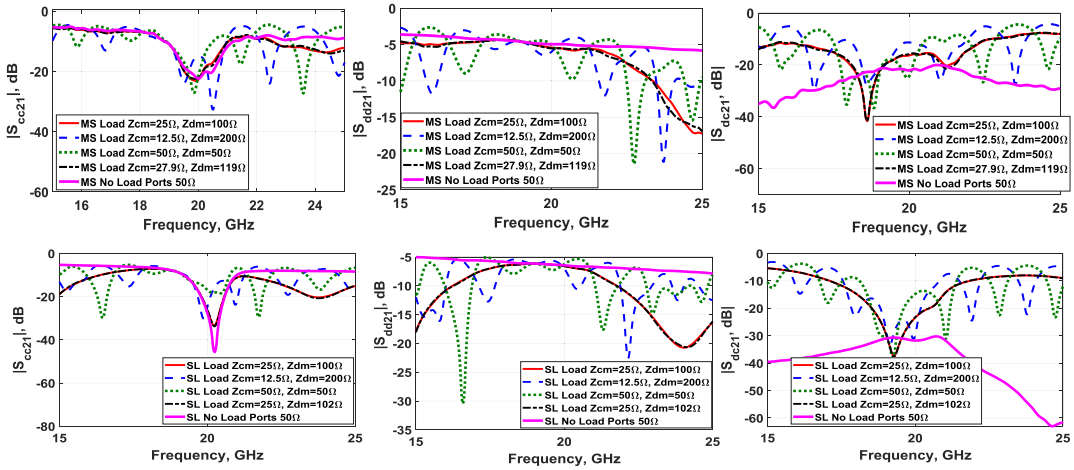

Fig. 19. Effects of unmatched load cascaded with EBG structures—MS (top row) and SL (bottom row) EBG.

characteristics is imperative for a PCB high-speed electronics designer.

VI. Conclusion

The impedance mismatch effects on the characteristics of microstrip and stripline CM EBG filters are studied using 3-D full-wave numerical simulations based on the results of some models validated by measurements. It is shown that the lines impedance mismatch in MS and SL has different effects on the EBG CM filter characteristics. The mismatch effects appear to be stronger in the SL case than in the MS case. However, the deviations in the impedances of MS and SL differential pairs within ±25% from the nominal (matched) values do not drastically deteriorate the performance of the EBG CM filters. The CM notch frequency in the MS case practically does not vary (only slightly reduces within 30 MHz range for the considered range of impedances).

In the SL case, the variation in the CM notch frequency is slightly larger than in the MS case, but still is within 100 MHz range of variation. The intended bandwidth of the designed filters at −15 dB level is not less than 1 GHz. This requirement has been satisfied even for the SL filters with the lowest of the considered trace width of $wt = 0.08$ mm. Bandwidth at −15 dB level of both MS and SL CM filters increases as mismatch increases, and this is the favorable effect. The notch depth behaves differently in MS and SL cases. However, if below the −15 dB, the value of the notch depth does not matter from the CM mitigation point of view as soon as the sufficient filter bandwidth at the required frequency is achieved.

It is also shown that the lower port impedances (<50 Ω) may have significant effect on the characteristics of the CM EBG filters. In addition, if EBG filters are cascaded with significantly unmatched four-port load, this may also deteriorate performance of filters. Therefore, characteristics of EBG filters are comparatively robust to technological deviations in widths of the traces and separation distances in differential pairs. However, strong mismatching with loads and/or network port impedances may be undesirable, especially from SI point of view.

Note that skew in a differential pair may also affect the CM notch filter parameters. Such study was done in the article [5], where line length imbalance effects in the same MS and SL EBG filters were quantified. As is seen by comparing Fig. 16 in [5] with Figs. 7, 8, 12, and 13 in this paper, the line length imbalance effect (and hence the corresponding skew) may be comparable and even stronger than the effects of impedance mismatch (at least within technological tolerances), especially for MS EBG structures. However, in practical designs, skew is typically known and can be compensated by a proper PCB layout design.

Though the analysis has been done for 20-GHz CM EBG filters, the modeled trends should serve as guidelines for the similar rectangular patch-type filters designed for other multi-GHz frequencies—see the design methodology in [3]–[5].

References

[1] A. Orlandi, B. Archambeault, F. de Paulis, and S. Connor, *Electromagnetic Bandgap (EBG) Structures: Common-Mode Filters for High Speed Digital Systems*. New York, NY, USA: Wiley, 2017.

[2] M. Pajovich, J. Savic, A. Bhobe, and X. Zhou, "The gigahertz two-band common-mode filter for 10-Gbit/s differential signal lines," in *Proc. IEEE Symp. Electromag. Compat.*, Aug. 2013, pp. 472–477.

[3] M. Koledintseva, S. Radu, and J. Nuebel, "Physical and technological aspects of microstrip EBG filter design," in *Proc. IEEE Int. Symp. Electromagn. Compat., Signal Integrity Power Integrity*, Jul./Aug. 2018, pp. 211–216.

[4] M. Koledintseva, S. Radu, and J. Nuebel, "Design and sensitivitry analysis of EBG stripline common-mode filters," *IEEE Trans. Electromagn. Compat.*, vol. 61, no. 6, pp. 1746–1759, Dec. 2019.

[5] M. Y. Koledintseva, S. Radu, and J. Nuebel, "EBG common-mode 20-GHz microstrip and stripline filters: Sensitivity to design parameters," *IEEE Trans. Electromag. Compat.*, to be published, doi: 10.1109/TEMC.2019.2950019.

[6] 3DS CST Studio Suite – Electromagnetic Field Simulation Software, "Dassault systems simulia," 2020. [Online]. Availabe: https://www.3ds.com/products-services/simulia/products/cst-studio-suite/

[7] M. Koledintseva, T. Vincent, A. Ciccomancini Scogna, and S. Hinaga, "Method of effective roughness dielectric in a PCB: measurement and full-wave simulation verification," *IEEE Trans. Electromag. Compat.*, vol. 57, no. 4, pp. 807–814, Aug. 2015.

[8] Y. Kayano, M. Ohkoshi, and H. Inoue, "Weak-coupled cross-sectional differential-paired lines with bend discontinuities for SI and EMI performances," in *Proc. IEICE Int. Conf.*, May 2014, pp. 133–136.

[9] M. Koledintseva, S. Radu, and J. Nuebel, "Impedance mismatch effects in microstrip and stripline EBG common-mode filters," in *Proc. IEEE Symp. EMC+SIPI*, Jul. 2019, pp. 372–377.

[10] Impedance Calculators, EE Web Tools, *AspenCore, Inc.*, 2020. [Online]. Availabe: https://www.eeweb.com/tools

Marina Y. Koledintseva (Senior Member, IEEE) received the M.S.E.E. and Ph.D.E.E. degrees from Moscow Power Engineering Institute—National Research University, Moscow, Russia, in 1984 and 1996, respectively.

From 1996 to 2000, she was a Research Scientist and an Associate Professor with the National Research University. In January 2000, she joined EMC Lab of Missouri University of Science and Technology (former UMR) , where she worked as a Research Professor of electrical engineering till April 2014. Then, from 2014 to 2018, she was a Principal Hardware Design Engineer with Electromagnetic Compatibility group with Oracle Corp. USA. In September 2018, she joined Metamagnetics, Inc., USA, as a Technical Director of R&D. She is an author of 260 publications, including book chapters, peer-reviewed journal articles, international symposia and conference proceedings, and seven inventions. Her research interests include electromagnetic compatibility and signal integrity in electronic systems; computational electromagnetics; development of analytical and numerical models and experimental methodologies to study complex electromagnetic structures and advanced materials; and using various physical phenomena in materials to design new microwave devices, including microwave magnetic ICs.

Dr. Koledintseva was the recipient of numerous best paper awards of international symposia and journals, including the IPC APEX EXPO Best Technical Paper Award in 2009, 2010, and 2018; IEEE TRANSACTION ON EMC Honorable Paper Mention Award in 2015, and IEEE EMC Symposium Best Paper Award in 2012 and 2014. From 2007 to 2010, she was a Secretary of Technical Committee TC-11 "Nanotechnology and Advanced Materials" of IEEE EMC-S; in 2010-2014 served as a Chair of TC-11, and since 2018, she has been a Vice-chair of TC-11.

Sergiu Radu (Senior Member, IEEE) received the M.S. and Ph.D. degrees in electrical engineering (electronics) from the Technical University of Iasi, Iasi, Romania, in 1980 and 1995, respectively.

He was an Associate Professor at the Technical University of Iasi until 1996, involved in Electromagnetic Compatibility teaching and research. From 1996 to 1998, he was a Visiting Scholar with the University of Missouri at Rolla, currently Missouri University of Science and Technology, as part of the Electromagnetic Compatibility Laboratory. In 1998, he joined the Electromagnetic Compatibility Engineering group at Sun Microsystems, which became a part of Oracle Corp. in 2010. He is currently the Director of Hardware Development with Oracle leading the EMC Design group in Santa Clara, CA, USA, involved in chassis level, PCB level and chip level EMC design for all Oracle hardware products. His role includes also the development and implementation of platform level EMC Design architecture, design methodologies, and better EMC prediction techniques. He holds seven US patents for EMI reduction techniques in electronic systems and has authored or coauthored more than 50 technical papers, presentations and reports on electromagnetic compatibility related subjects.

Dr. Radu is NARTE Certified Engineer since February 1998, a former IEEE EMC Distinguished Lecturer (2009-2010), and a reviewer for IEEE TRANSACTIONS ON EMC.

Joe Nuebel (Member, IEEE) received the AASEE degree in electrical engineering with Hawkeye Institute of Technology, Waterloo, ON, Canada, in 1978.

For the past 32 years he has been working for Sun Microsystems and then Oracle Corp. (as Sun became a part of Oracle Corp. in 2010) first in the Compliance department and then in the EMC Hardware Design group. He is currently a Principal Hardware Engineer with EMC Design, Oracle. His EMC product design contribution has included everything from high speed switches and large multisocket servers to disk drives and PCIe cards.